Doonan *et al.* Supplemental Material

Molecular and biochemical characterization of *sod* mutants

To try to understand why *C. elegans* has so many SOD isoforms, we characterized expression of each of the five *sod* genes. This analysis included the use of deletion alleles for each *sod* gene (Figure S1A) obtained from the NBP-Japan (for which we thank S. Mitani) or the *C. elegans* Knockout Consortium (for which we thank D. Moerman). All mutations were backcrossed at least four times to N2. All *sod* mutants studied are viable, and all contain null alleles based on the following evidence.

The deletion *sod-1(tm776)* (Figure S1A) results in a frameshift following amino acid 44 (based on ORF C15F1.7a; WormBase) eliminating 75% of the protein, including all residues mediating coordination of the metal cofactors. Furthermore, Cu/ZnSOD protein is not detectable in the *sod-1* mutant (Figure S1C), total SOD activity is reduced by around 80% (Figure S1D,E) and the mutant is hypersensitive to paraquat-generated O_2^- (Figure 2A). The deletion *sod-5(tm1146)* results in a frameshift following amino acid 25, eliminating 86% of the wild-type protein, including all residues mediating coordination of the metal cofactors.

The deletion *sod-4(gk101)* results in a frameshift following amino acid 20, eliminating 89% of the protein, including most of the residues mediating coordination of the metal cofactors.

sod-2(gk257) is a short deletion eliminating the first exon (Figure S1A), which encodes the N-terminal mitochondrial targeting signal. Although the deletion probably does not eliminate the *sod-2* transcriptional start site, the first available translational start site (ATG) is out of frame. Consistent with this, we detect no MnSOD protein in *sod-2* mutants (Figure S1C). The *sod-3(tm760)* deletion results in a frameshift following amino acid 17, eliminating 92% of the SOD-3 protein, including all residues mediating coordination of the metal cofactor.

***sod-1* and *sod-2* encode the major Cu/ZnSOD and MnSOD isoforms**

sod-1 and *sod-5* encode putative cytosolic Cu/ZnSOD genes. In wild-type adults, *sod-1* is highly expressed, representing approximately 76% of all *sod* mRNA (Figure S1B). Consistent with this, Cu/ZnSOD protein (as detected by Westerns) is below the level of

detection in *sod-1* mutants (Figure S1C). Furthermore, *sod-1(0)* decreases total SOD activity by ~80% (Figure S1D,E). Thus, *sod-1* contributes most of the total SOD activity in *C. elegans,* consistent with an earlier observation (Jensen and Culotta 2005). By contrast, *sod-5* mRNA is only 0.5% of all *sod* mRNA (Figure S1B), and *sod-5(0)* has no detectable effect on Cu/ZnSOD protein level or total SOD activity (Figure S1C,D,E).

To characterize further the expression of *sod-1* and *sod-5,* we fused the green fluorescent protein (GFP) to the C-terminus of each protein (Figure S2) and examined tissue specificity and cellular localization of the fusion protein. *sod-1::gfp* expression was ubiquitous in somatic cells in L3 larvae (Figure S4C) and all other post-embryonic stages (data not shown). Expression was marked in the terminal bulb of the pharynx, intestinal cells (Figure S4C), and in the ADL, ASI and ASK amphid neurons (Figure S3A). Strong *sod-5::gfp* expression was also seen in ASI and ASK, and also ASG (Figure S3B,C), but almost nowhere else (Figure S4D).

sod-5::gfp expression in ASI, ASK and ASG showed substantial inter-individual variation in expression level despite chromosomal integration of the transgene. This probably reflects stochastic variation in ontogenic and/or microenvironmental factors (Krause et al. 1994; Rea et al. 2005). This variable expression was suppressed by loss of *daf-16* (Figure S4D), suggesting that the extent of *sod-5::gfp* distribution may reflect stochastic, inter-individual variation in levels of DAF-16 activation. Possibly, such variation contributes to the surprising variation in individual lifespan in isogenic *C. elegans* populations.

We studied Cu/ZnSOD protein levels and subcellular distribution in *C. elegans* using an anti-Cu/ZnSOD antibody and *sod::gfp* transgenic lines. To confirm the specificity of the antibody, *sod-1*, *sod-4* and *sod-5* cDNAs were cloned into a pET-3a vector and over-expressed in BL21(DE3) plysS *E. coli* cells (Invitrogen, Carlsbad, CA, USA). The Cu/ZnSOD antibody was equally reactive against all three recombinant Cu/ZnSOD proteins (data not shown).

Western blot analysis shows that Cu/ZnSOD protein is largely present in the cytosolic fraction, confirming that in *C. elegans* Cu/ZnSOD (presumably SOD-1) is a cytosolic enzyme (Figure 3A). However, in the *sod-1* over-expressing strain, Cu/ZnSOD immunoreactivity was also detected in the mitochondrial fraction, which likely reflects the presence of this enzyme in the mitochondrial inter-membrane space (Figure 3A).

Antibody to the cytosolic protein actin did not bind to the mitochondrial fraction (Figure 3A), ruling out the possibility that the presence of Cu/ZnSOD in the mitochondrial fraction was due to contamination with cytosolic proteins.

sod-1::gfp shows a diffuse pattern of localization consistent with SOD-1 being a cytosolic SOD (Figure S4C). GFP expression level was quite variable, despite integration of the *sod-1::gfp* transgene (data not shown). In addition to the expression seen in the terminal bulb of the pharynx, the anterior and posterior ends of the intestine, and the ASI and ASK amphid neurons, there is also expression in the phasmid neurons, the lateral CAN neurons and, variably, the distal tip cells.

In addition to the strong expression in amphid neurons, weak *sod-5::gfp* expression is visible throughout the intestine, particularly at the anterior and posterior ends but, unlike *sod-1::gfp*, not in the pharynx, and in the CAN neurons. Given that *sod-5* mRNA levels are very low in non-dauer, wild-type *C. elegans* (Figure S1B), it seems possible that some of this *sod-5::gfp* expression is artefactual, particularly in the posterior intestine. Inappropriate reporter expression in the posterior intestine has been seen for other genes (Krause et al. 1994), and might be caused by the *unc-54* 3' UTR in the plasmid constructs used.

Turning to MnSOD, *sod-2* mRNA is highly expressed in wild-type adults, representing approximately 18% of total *sod* mRNA, whereas *sod-3* contributes only 1% of total *sod* mRNA (Figure S1B), consistent with previous findings (Honda and Honda 1999). Moreover, MnSOD protein (i.e. SOD-3) was not detected in *sod-2* mutants (Figure S1C). Thus, SOD-2 is the main MnSOD isoform in *C. elegans*. However, we did not detect a reduction in total SOD activity in *sod-2* mutants (Figure S1D).

We also examined lines bearing integrated *sod-2::gfp* and *sod-3::gfp* transgenes (Figure S2), and both showed marked expression in the pharynx (Figure S3D,E). SOD-2::GFP expression was most marked in the procorpus and, particularly, the terminal bulb region of the pharynx (Figure S3D), intestinal cells, and various hypodermal cells (data not shown). This could reflect a high level of metabolic activity and/or mitochondria at these sites. Faint expression was also visible in some neurons anterior to the pharynx, and in the posterior intestine (data not shown). The fact that SOD-2::GFP was not visible in all cells could imply that mitochondria in some cells do not contain SOD-2, or that some cells have very few mitochondria. Alternatively, expression of *sod-2::gfp* may not

fully recapitulate native *sod-2* gene expression. Surprisingly, *sod-3::gfp* was highly expressed in fully-fed larvae, in a pattern similar to that of *sod-2::gfp* (Figure S3E). This similarity suggests that *sod-2* and *sod-3* share common promoter elements. However, given that very little *sod-3* mRNA is detected in wild-type adults, either by us or others (Honda and Honda 1999), the high level of *sod-3::gfp* expression seems likely to be artefactual.

Western blot analysis shows that MnSOD protein is limited to mitochondria, confirming that in *C. elegans* MnSOD (presumably SOD-2) is a mitochondrial enzyme (data not shown). Consistent with this, we observed punctate co-localization of SOD-2::GFP and the mitochondrial dye MitoTracker in the intestine (data not shown). MitoTracker staining was not seen in most parts of the worm anatomy (e.g. the pharynx), probably due to resistance of *C. elegans* to dye uptake.

Overall, these results show that SOD-1 and SOD-2 are the main cytosolic Cu/ZnSOD and mitochondrial MnSOD isoforms, respectively. By contrast expression of *sod-5* and *sod-3* is very low and/or spatially restricted in fully-fed, wild-type *C. elegans*.

sod-5 and _sod-3_ encode dauer-up-regulated CuZnSOD and MnSOD isoforms

Next we explored the expression of *sod* genes in dauer larvae, starting with an examination of mRNA levels. Compared to adults, in dauers *sod-1* and *sod-2* mRNA copy numbers decrease by 7- and 8-fold, respectively, while, *sod-5* and *sod-3* mRNA copy numbers increase by 13- and 2-fold, respectively (Figure S4A). Yet despite the high level of *sod-5* mRNA in dauers, Cu/ZnSOD protein was detected in *sod-5(0)* but not *sod-1(0)* dauers (Figure S1C). Moreover, *sod-1(0)* but not *sod-5(0)* reduces SOD activity in dauer larvae (Figure S1D). Thus, we do not detect an increase in SOD-5 protein corresponding to the elevation of *sod-5* mRNA levels in dauers. Similarly, despite elevated levels of *sod-3* mRNA in dauers (Figure S1B), *sod-2(0)* eliminates detectable MnSOD protein (Figure S1C).

Expression of *sod::gfp* translational fusions confirmed elevated levels of *sod-5* and *sod-3* in dauer larvae (Figure S4B,D,F). Bright, punctate SOD-3::GFP expression was seen throughout the animal, particularly in the terminal bulb and anterior portion of the pharynx (Figure S4F). Dauers also showed a striking striated pattern of *sod-3::gfp* fluorescence in or close to the cuticle, apparently corresponding to the cuticular alae; this

was also seen in starved L3 larvae (data not shown). For *sod-2::gfp*, the major sites of expression in dauer larvae were, as in wild-type L3s, in the pharynx and intestine. However, in dauer larvae, the level of intestinal expression was much higher than in the pharynx, whereas in L3s the opposite was the case.

Overall, our results imply that although *sod-5* and *sod-3* mRNA levels are elevated in dauer larvae, SOD-1 and SOD-2 remain the predominant cytosolic Cu/ZnSOD and mitochondrial MnSOD isoforms, respectively.

Expression of the *sod-4* extracellular Cu/ZnSOD

sod-4 contributes 5% of all *sod* mRNA in wild-type adults, but 20% in dauer larvae (Figure S1B), suggesting that this isoform is particularly important during the dauer stage. Consistent with this, we detected no change in overall SOD activity in *sod-4(0)* adults, but slightly reduced activity in *sod-4(0)* dauer larvae, though this decrease was not statistically significant (Figure S1D). Unfortunately, GFP was not detected in any of our *sod-4::gfp* lines, even in dauer larvae, perhaps because the extracellular localization of SOD-4 leads to overly diffuse GFP.

One possibility is that the SOD-4 extracellular Cu/ZnSOD is secreted out of *C. elegans* and into the culture medium, as occurs in some other nematodes. For example, parasitic *Brugia malayi* lymphatic filariasis nematodes secrete Cu/ZnSOD to protect themselves against superoxide produced by host leukocytes (Ou et al. 1995). To test this we compared SOD activity levels in culture medium from wild-type and *sod-4* mutant adult populations, but the levels did not differ (data not shown). We also compared culture medium from *sod-1* and *sod-1; sod-4* populations, but SOD activity levels were undetectably low in both cases (data not shown). This suggests that *C. elegans* does not secrete significant amounts of SOD-4 into the surrounding environment.

***sod* expression in *daf-2* mutants**

Previous work has shown that in *daf-2* mutants, there is an elevation in levels of SOD activity (Vanfleteren 1993) and *sod-3* mRNA (Honda and Honda 1999; Yanase et al. 2002). We examined the effect of *daf-2* on expression of the five *sod* genes. In *daf-2* mutants, as in wild type, the level of *sod-1* mRNA greatly exceeds that of *sod-5* (Figure S1B). By contrast, *sod-2* and *sod-3* mRNA levels are similar in *daf-2* mutants, as in

dauers (Figure S1B). qPCR analysis detected an increase in *sod-3* mRNA in *daf-2* relative to wild-type adults (Figure S4A). Examination of published microarray data comparing *glp-4; daf-2* relative to *daf-16 glp-4; daf-2* mutants (McElwee et al. 2004) showed significant increases not only of *sod-3* mRNA (17.7-fold), but also *sod-1* (1.7-fold) and *sod-5* mRNA (3.1-fold).

Next we compared levels of SOD::GFP protein in wild-type, *daf-2* and *daf-16; daf-2* backgrounds. Consistent with mRNA data, SOD-1::GFP, SOD-3::GFP, and SOD-5::GFP levels are all elevated by *daf-2* (Figure S4B). This effect is *daf-16* dependent in the case of *sod-3* and *sod-5* but, surprisingly, not *sod-1* (Figure S4B). *daf-2(m577)* had little effect on *sod-2::gfp* expression.

We also examined the contribution of each *sod* gene to total SOD activity in *daf-2* mutants. Again, only *sod-1(0)* causes a large and significant decrease in SOD activity level (Figure S1E). Consistent with this, we do not detect Cu/ZnSOD protein in *sod-1; daf-2* adults (Figure S1C). Thus, SOD-1 is the main cytosolic Cu/ZnSOD in *daf-2* mutants. With respect to MnSOD, despite *sod-3* up-regulation in *daf-2* mutants, SOD-2 is clearly the main MnSOD (Figure S1C). However, uniquely, we can detect a low level of MnSOD protein, presumably SOD-3, in *sod-2; daf-2* adults (Figure S1C).

Of the five *sod* genes, *sod-5* and *sod-3* show clear IIS-regulation of spatial expression. The expression of *sod-5::gfp* in the ASK, ASI, and ASG amphid neurons (see above) is greatly elevated by *daf-2*, and abrogated by *daf-16; daf-2* (Figure S4D). *sod-3::gfp* expression is up-regulated in intestinal cells of *daf-2* mutants and this is *daf-16* dependent (Figure S4F), consistent with previous findings (Libina et al. 2003; Chavez et al. 2007).

Age increase in molecular damage not detected in *sod-1* mutant

The shorter lifespan of *sod-1* mutants could reflect an acceleration of aging, or effects of pathology unrelated to aging. To try to distinguish these possibilities, we tested whether the rate of accumulation with increasing age of molecular damage is accelerated by the *sod-1* mutation. Age-related increases in molecular damage are a hallmark of biological aging. We tested whether *sod-1* mutants display more oxidation of lipid or protein relative to age-matched controls, examining populations at early, mid and late life. Protein oxidation was estimated by measuring activity levels of cytosolic or mitochondrial aconitase; aconitase is an iron-sulfur protein that is particularly sensitive to

inactivation by oxidation. No acceleration in accumulation of molecular damage was detected in *sod-1* mutants (data not shown). This could imply either that the shortening of lifespan of *sod-1* mutants is not due to accelerated aging, or merely that such an acceleration was too subtle for us to detect.

Increased temperature elevates *sod-1* expression

Total SOD activity level was affected by temperature. Levels were similar at 17˚C and 20˚C, but ~30% higher at 24˚C (Figure S6A). This increase did not reach statistical significance ($p = 0.11$), perhaps due to high variance between individual estimates. Loss of *sod-1* abrogated this effect (Figure S6A), implying that it is attributable to the effects of temperature on *sod-1* expression. The temperature sensitivity was not dependent on the DAF-16 and HSF-1 transcription factors (data not shown). Temperature had no effect on *sod-1* mRNA levels (Figure S6B), but SOD-1::GFP levels increased significantly with increasing temperature (Figure S6C). This suggests that the effect of temperature on *sod-1* expression is exerted at the post-transcriptional level. Possibly, the temperature sensitivity of *sod-1* expression reflects an increase in O_2^- levels with increasing temperature. Levels of catalase activity were also higher at higher temperatures (data not shown).

Fusion to GFP reduces SOD-1 specific activity

To test whether fusion of GFP to SOD-1 reduced specific activity of the enzyme, we first asked whether the *sod-1::gfp* transgene could rescue the shortened lifespan phenotype of *sod-1* mutants, and found that it could (data not shown). This demonstrates that SOD-1::GFP has at least some SOD activity. However, SOD activity assays of protein extracts from SOD-1::GFP did not detect any increase in SOD activity relative to wild type (data not shown), suggesting that SOD-1::GFP might indeed have low specific activity. To test this, we used an in situ gel SOD activity assay to compare protein extracts from wild type and *sod-1::gfp* transgenic *C. elegans*. In the latter an additional, high running band of SOD activity was seen, but it was markedly weaker than the endogenous SOD activity band (Figure S7). In a Western blot using an anti-GFP antibody, extracts from the SOD-1::GFP showed a high running band at the same position as the high-running, weak SOD activity band (Figure S7), confirming that the latter corresponded to the SOD-1::GFP

fusion protein. Given that SOD-1::GFP is highly expressed in the transgenic strain, and copy number of the *sod-1::gfp* transgene is likely to greatly exceed that of the endogenous *sod-1* gene, it is probable that levels of SOD-1::GFP exceed those of endogenous SOD-1. This being so, the above tests imply that the SOD specific activity of the SOD-1::GFP fusion protein is low.

Supplemental References

Chavez, V., Mohri-Shiomi, A., Maadani, A., Vega, L.A., and Garsin, D.A. 2007. Oxidative stress enzymes are required for DAF-16-mediated immunity due to generation of reactive oxygen species by *Caenorhabditis elegans*. *Genetics* **176**: 1567-1577.

Honda, Y. and Honda, S. 1999. The *daf-2* gene network for longevity regulates oxidative stress resistance and Mn-superoxide dismutase gene expression in *Caenorhabditis elegans*. *FASEB J* **13**: 1385-1393.

Jensen, L.T. and Culotta, V.C. 2005. Activation of CuZn superoxide dismutases from *Caenorhabditis elegans* does not require the copper chaperone CCS. *J Biol Chem* **280**: 41373-41379.

Krause, M., Harrison, S.W., Xu, S.Q., Chen, L., and Fire, A. 1994. Elements regulating cell- and stage-specific expression of the *C. elegans* MyoD family homolog *hlh-1*. *Dev Biol* **166**: 133-148.

Libina, N., Berman, J., and Kenyon, C. 2003. Tissue-specific activities of *C. elegans* DAF-16 in the regulation of lifespan. *Cell* **115**: 489-502.

McElwee, J.J., Schuster, E., Blanc, E., Thomas, J.H., and Gems, D. 2004. Shared transcriptional signature in *C. elegans* dauer larvae and long-lived *daf-2* mutants implicates detoxification system in longevity assurance. *J Biol Chem* **279**: 44533-44543.

Ou, X., Tang, L., McCrossan, M., Henkle-Dührsen, K., and Selkirk, M.E. 1995. *Brugia malayi*: Differential expression of extracellular and cytoplasmic CuZn superoxide dismutases in adult and larval stages. *Exp Parasitol* **80**: 515-529.

Rea, S.L., Wu, D., Cypser, J.R., Vaupel, J.W., and Johnson, T.E. 2005. A stress-sensitive reporter predicts longevity in isogenic populations of *Caenorhabditis elegans*. *Nat Genet* **37**: 894-898.

Vanfleteren, J.R. 1993. Oxidative stress and ageing in *Caenorhabditis elegans. Biochem J* **292**: 605-608.

Yanase, S., Yasuda, K., and Ishii, N. 2002. Adaptive responses to oxidative damage in three mutants of *Caenorhabditis elegans* (*age-1, mev-1* and *daf-16*) that affect life span. *Mech Ageing Dev* **123**: 1579-1587.

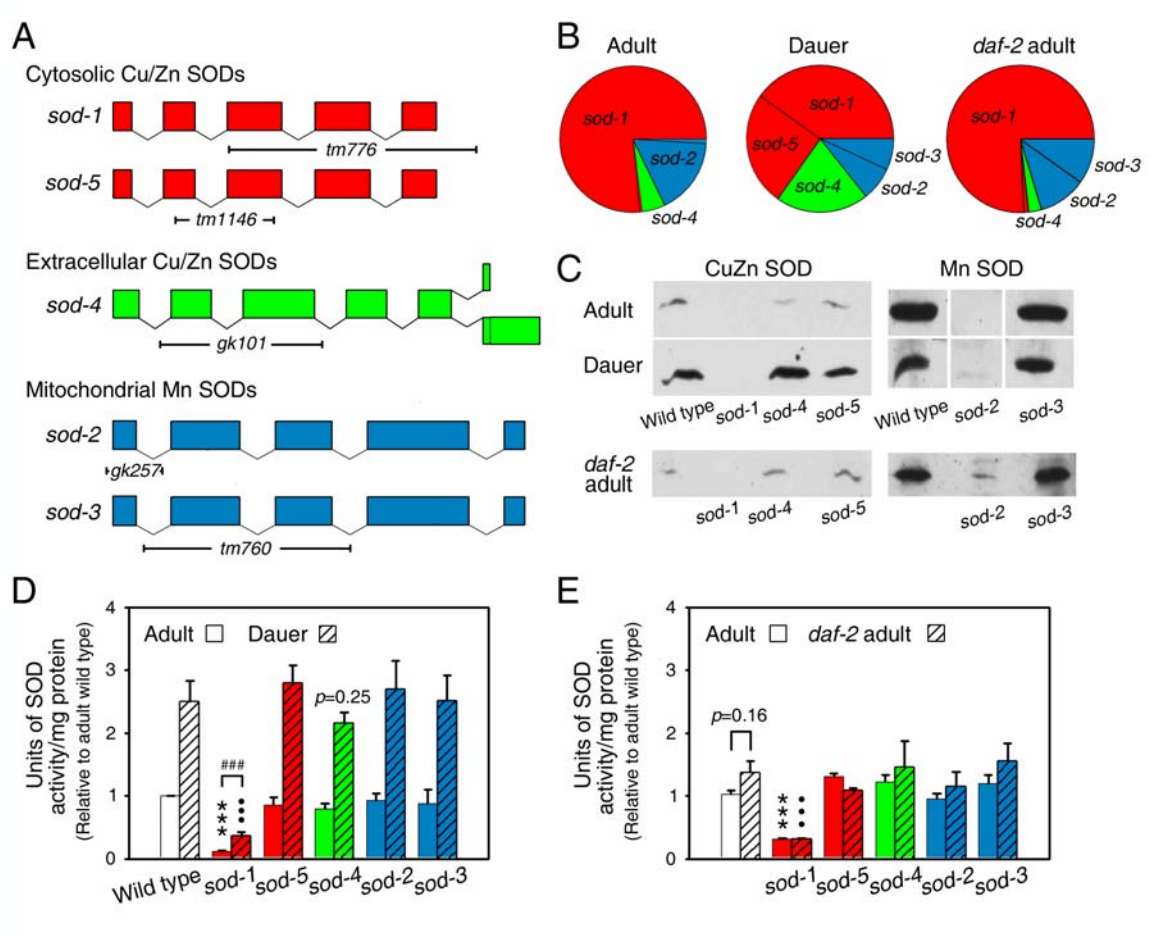

Figure S1. Expression of *sod* genes. (A) Deletion mutations in *sod* genes. Exons are represented as boxes linked by introns. Exons but not introns are to scale. For a detailed description of each mutation, see Supplemental Material. (B) mRNA expression level of each *sod* gene presented as proportion of total *sod* mRNA, in wild-type adults, wild-type dauer larvae and *daf-2* adults, as estimated by RT-PCR. (C) Western blots of total protein extracts from *sod* mutants. Protein from adults and dauer larvae was run simultaneously with equal loading and can therefore be compared directly; equality of protein loading was assured by staining with a reversible protein dye (MemCode, Thermo Fisher Scientific Inc., Rockford, IL, USA). *daf-2* mutant blots were run independently. (D,E) Total SOD activity in protein extracts from *sod* mutants. (D) Adults (open bars) and dauers (hatched bars). *** indicates p <0.0001, *sod-1* adult vs. wild-type adult; ••• indicates p <0.0001, *sod-1* dauer vs. wild-type dauer; ### indicates p <0.0001; Student's t test. (E) Wild-type (open bars) and *daf-2* (hatched bars) adults. *** indicates p < 0.0001, *sod-1* adult vs. wild-type adult; ••• indicates p <0.0001,

sod-1;daf-2 adult vs. *daf-2* adult; Student's t test. *daf-2* allele used in mRNA studies was *e1370*; for Westerns and activity assays, *m577*. Note color coding of SOD classes: cytosolic = red, extracellular = green, and mitochondrial = blue.

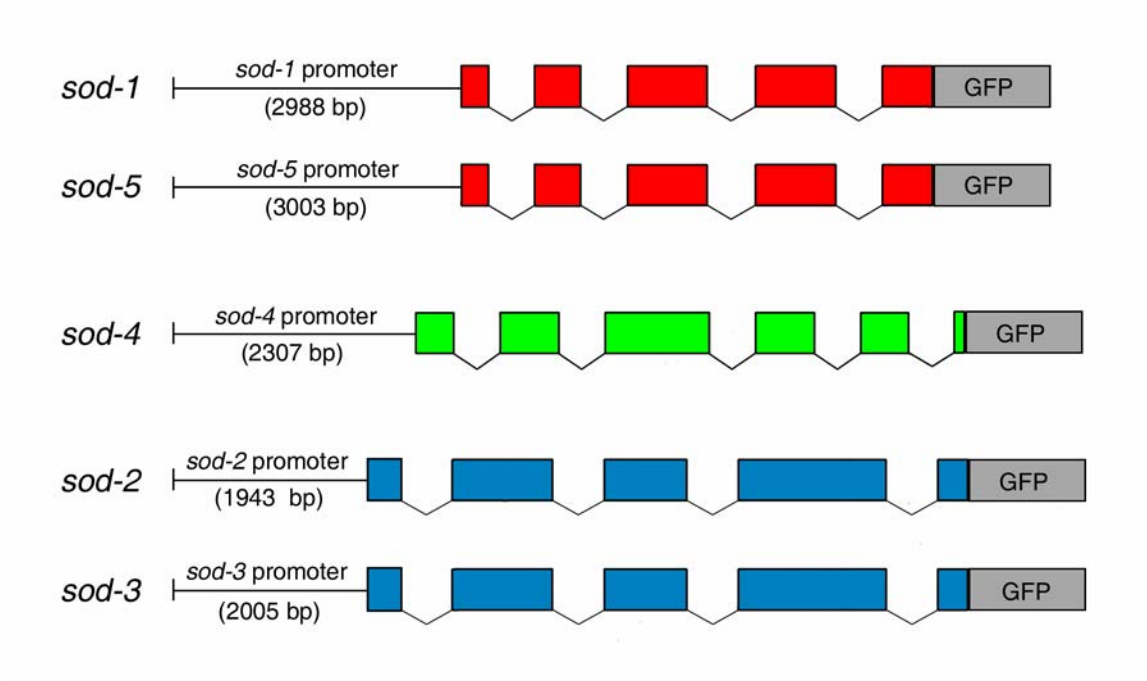

Figure S2. Constructs used for preparation of SOD::GFP transgenic lines. Plasmids containing the following constructs were injected into *C. elegans* to create lines expressing GFP-tagged SOD fusion proteins for each of the five *sod* genes. No GFP was detected in *sod-4::gfp* transformants.

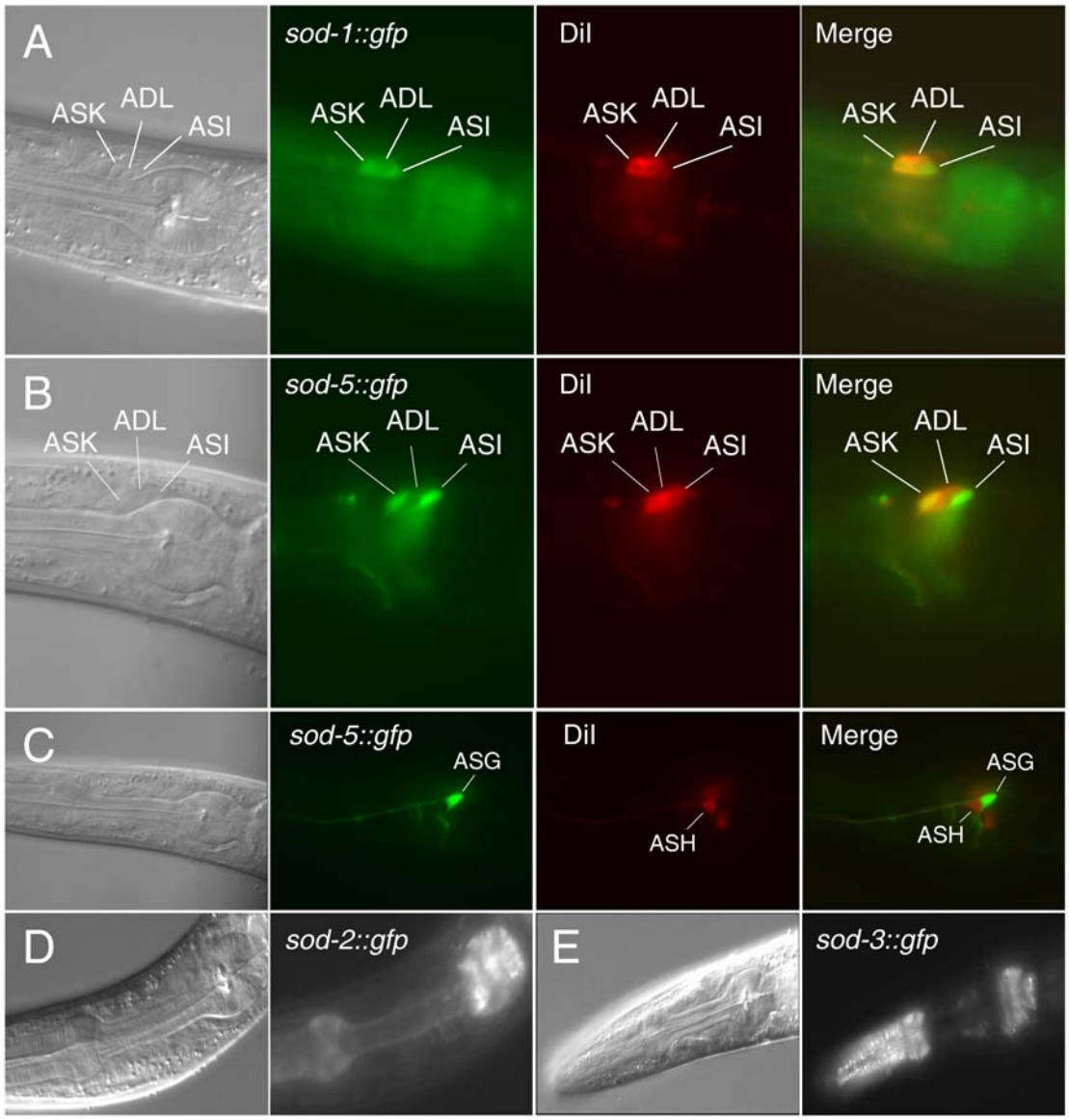

Figure S3. Expression of SOD::GFP fusion proteins. (A) *sod-1::gfp* expression in amphid neurons ASK and ASI. (B) *sod-5::gfp* expression in amphid neurons ASK and ASI. (C) *sod-5::gfp* expression in *daf-2(m577)* mutant in ASG amphid neuron. DiI is a fluorescent dye that stains many amphid neurons. (D, E) *sod-2::gfp* and *sod-3::gfp* expression in the pharynx. Anterior is to the left in each case.

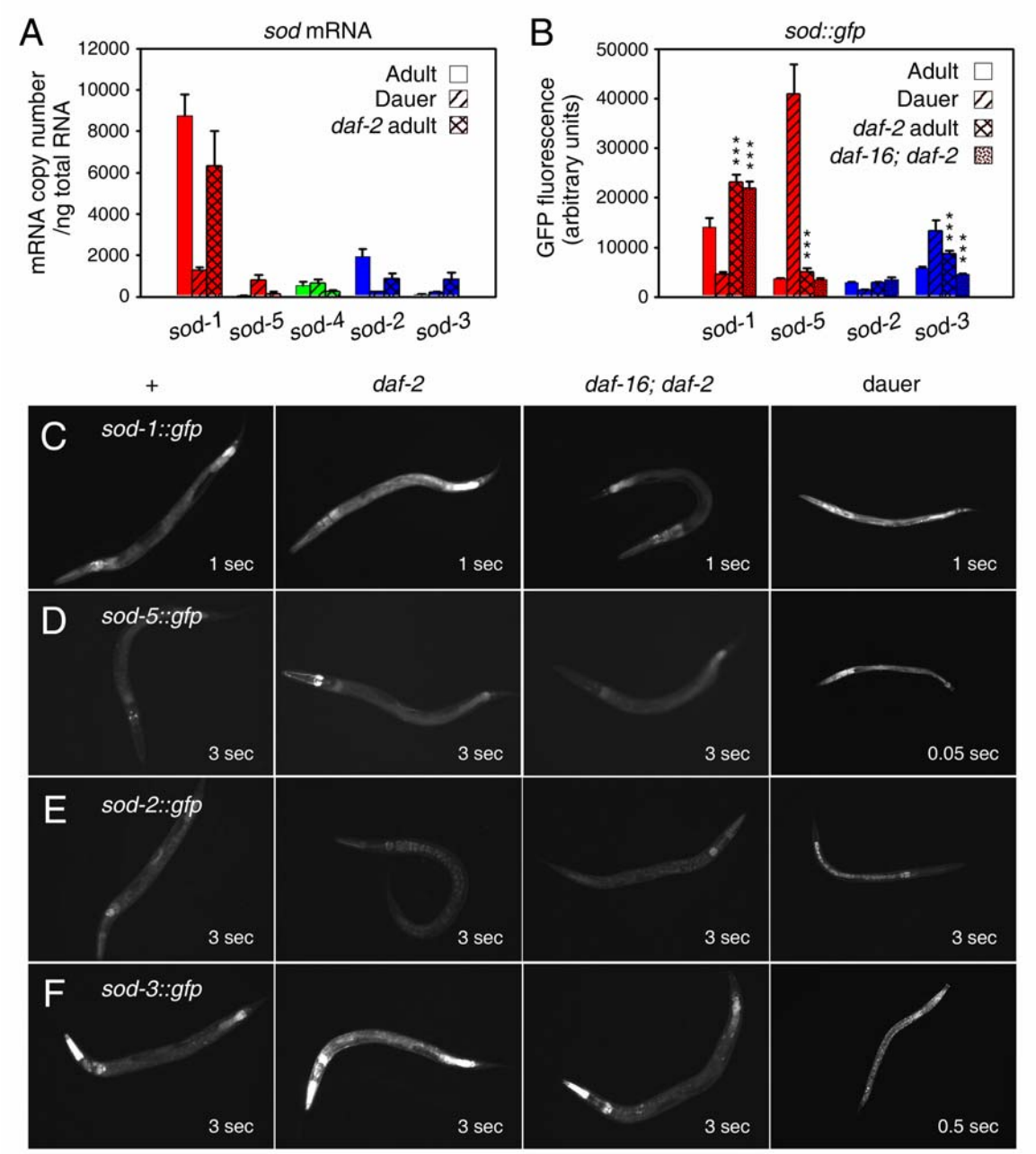

Figure S4. *sod-3* and *sod-5* upregulation in *daf-2* mutants is *daf-16* dependent. (A) Absolute *sod* mRNA copy number for all five *sod* genes in adults, dauers, and *daf-2* mutant adults. Note that transcription of *sod* genes is relatively low in dauers. (B) GFP fluorescence level as determined by spectrophotometry for all *sod::gfp* reporters in wild type adults, dauers, *daf-2* mutant adults, and *daf-16; daf-2* double mutants. Note that direct comparisons between reporters (e.g. *sod-1::gfp vs*. *sod-5::gfp*) cannot be made due

to differences in copy number and expression level of arrays. However, direct comparisons can be made for the same reporter in various genetic backgrounds (e.g. *sod-1::gfp* adults *vs. daf-2;sod-1::gfp* adults). Accordingly, *** indicates $p < 0.0001$ *vs.* respective *sod::gfp* adult. Note that the *sod-1*, *sod-3*, and *sod-5* reporters are up-regulated in *daf-2*, but only *sod-3* and *sod-5* up-regulation are *daf-16* dependent. (C-F) Expression pattern of *sod::gfp* reporters in wild type, *daf-2* and *daf-16; daf-2* mutant adults, and *daf-2(+)* dauer larvae resulting from population over-growth. Exposure time is indicated at the bottom right of each panel. *daf-2* allele is *m577*. *daf-16* allele is *mgDf50*.

Doonan et al. Figure S5

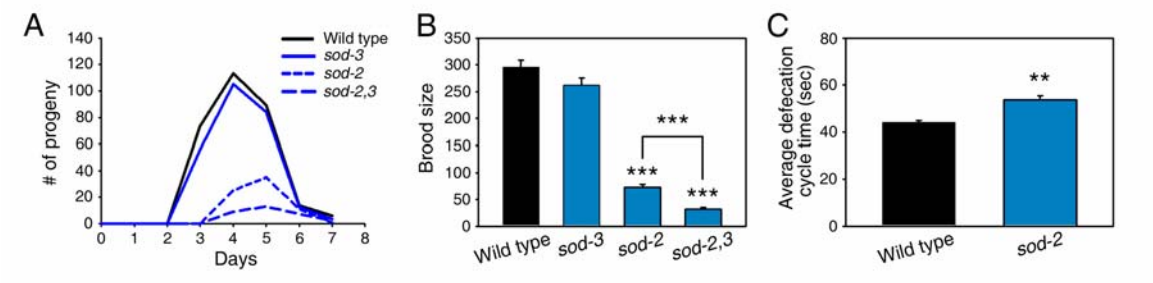

Figure S5. Effects of *sod-2(0)* and *sod-3(0)* on fertility and defecation. (A) Effects on reproductive schedule. (B) Effects on total brood size (lifetime fecundity). Data shows average of measurements of 15 unmated hermaphrodites for each genotype. (C) Effect of *sod-2(0)* on defecation cycle time (mean of defecation cycle time estimates for 14 animals in each case).

Doonan et al. Figure S6

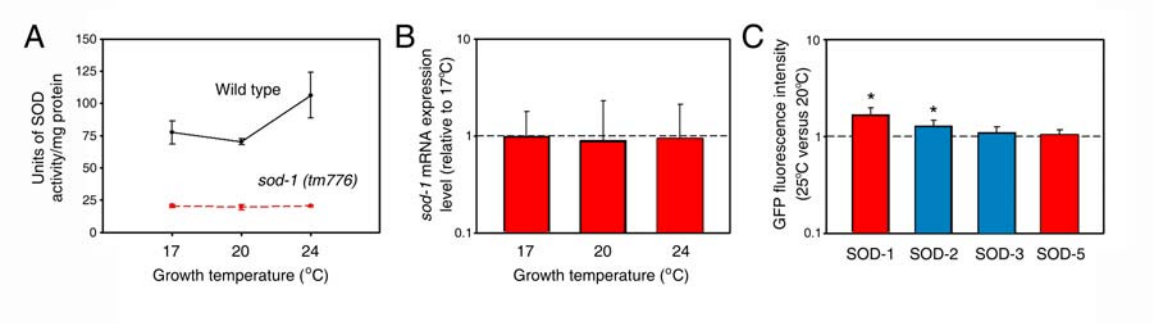

Figure S6. Effect of temperature on expression of *sod-1*. (A) Overall SOD activity. (B) *sod-1* mRNA levels. (C) SOD::GFP levels. The data suggests that increased temperature results increased expression of *sod-1* involving post-transcriptional regulation.

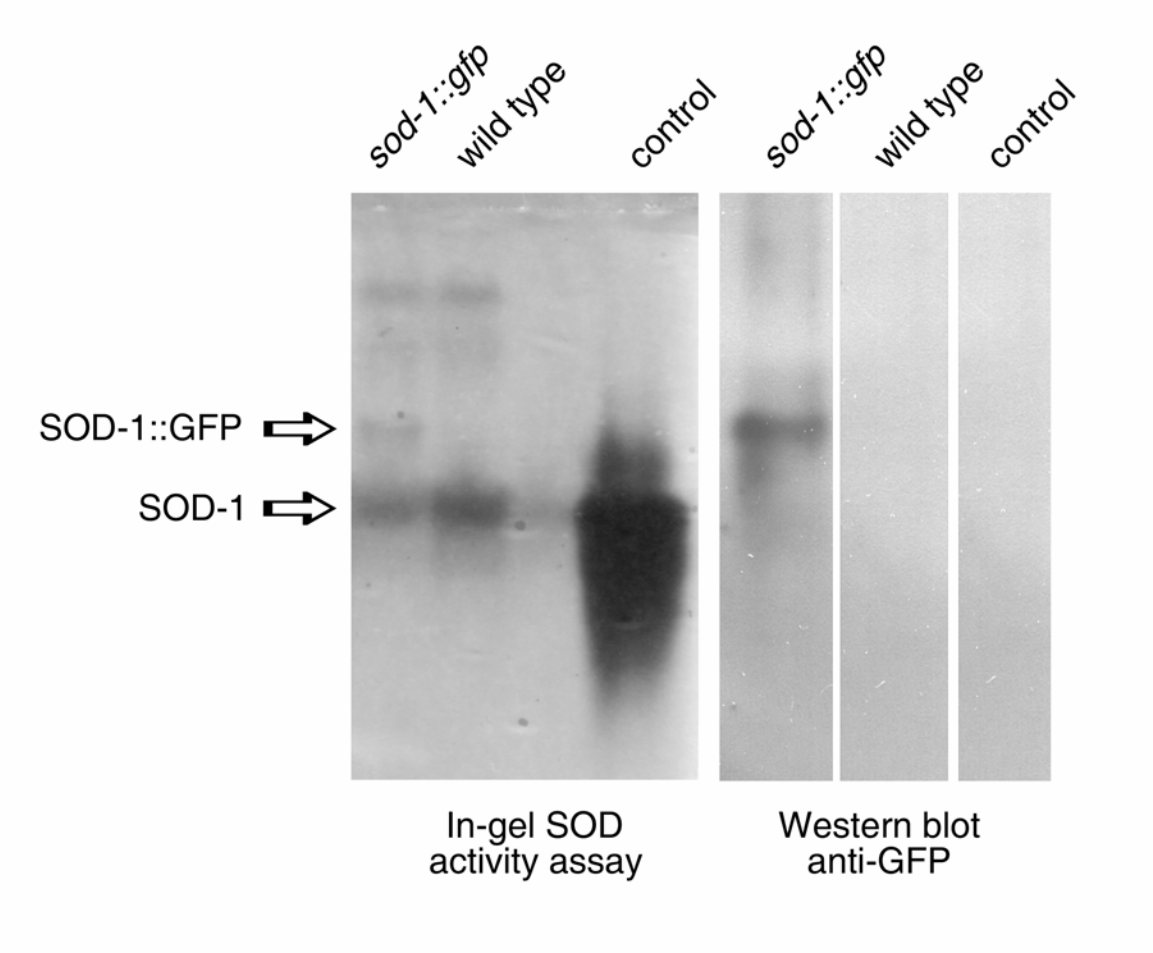

Figure S7. Analysis of specific activity of SOD-1::GFP. Right panel: In gel SOD activity assay (non-denaturing gel stained with nitro blue tetrazolium) using extracts from a strain containing the integrated transgene array *wuIs54* [*sod-1::gfp*] and wild type. A weak, high running band of approximately the predicted size of the SOD-1::GFP fusion protein is present in the *sod-1::gfp* line, but absent from the wild type. Left panel: Western analysis using an anti-GFP antibody revealed a similar size band in the *sod-1::gfp* line, but not the wild type. Control: mammalian (bovine) Cu/ZnSOD positive control.

Table S1

Effects of *sod* mutations on lifespan

Genotype [Trial number]	Temp.	Mean Lifespan[a]	% Change in lifespan	*n*[b]	*p*[c]
DATA IN FIGURES					
Wild type [1][d,e]	**20°C**	**19.6 ± 0.54**		**91**	
***sod-1* [1][d]**	**20°C**	**16.1 ± 0.35**	**-18**	**99**	**<0.0001**
***sod-2* [1][e]**	**20°C**	**19.4 ± 0.69**		**88**	
***sod-3* [1][e]**	**20°C**	**19.0 ± 0.43**		**89**	
***sod-4* [1][d]**	**20°C**	**18.8 ± 0.46**		**93**	
***sod-5* [1][d]**	**20°C**	**19.9 ± 0.54**		**69**	
Wild type [5][f,g]	**25°C**	**17.0 ± 0.47**		**60**	
***sod-1* [5][f]**	**25°C**	**13.0 ± 0.28**	**-24**	**57**	**<0.0001**
***sod-1 sod-5* [5][f]**	**25°C**	**11.9 ± 0.18**	**-16**	**57**	**<0.001**
***sod-2; sod-3* [5][g]**	**25°C**	**16.8 ± 0.46**		**60**	
ALL DATA					
Wild type [1]	20°C	19.6 ± 0.54		91	
Wild type [2]	25°C	14.2 ± 0.76		37	
Wild type [3]	25°C	16.0 ± 0.64		50	
Wild type [4]	25°C	12.6 ± 0.16		72	
Wild type [5]	25°C	17.0 ± 0.47		60	
Wild type [6]	25°C	16.7 ± 0.40		57	
Wild type [7]	20°C	19.0 ± 0.72		49	
sod-1 [1]	20°C	16.1 ± 0.35	-18	99	<0.0001
sod-1 [2]	25°C	9.8 ± 0.73	-31	39	<0.01
sod-1 [3]	25°C	11.3 ± 0.51	-29	51	<0.0001
sod-1 [4]	25°C	10.7 ± 0.16	-15	72	<0.0001
sod-1 [5]	25°C	13.0 ± 0.28	-24	57	<0.0001
sod-2 [1]	20°C	19.4 ± 0.69		88	
sod-2 [2]	25°C	13.1 ± 1.20		17	
sod-2 [3]	25°C	15.1 ± 0.80		57	
sod-2 [5]	25°C	14.8 ± 0.26	-13	60	<0.0001
sod-3 [1]	20°C	19.0 ± 0.43		89	
sod-3 [2]	25°C	16.0 ± 0.74		36	
sod-3 [3]	25°C	14.9 ± 0.62		52	
sod-3 [5]	25°C	14.6 ± 0.45	-14	60	<0.01
sod-4 [1]	20°C	18.8 ± 0.46		93	
sod-4 [2]	25°C	16.2 ± 1.00	+14	39	<0.01
sod-4 [3]	25°C	16.5 ± 0.96		32	
sod-4 [5]	25°C	13.5 ± 0.37	-21	60	<0.0001
sod-5 [1]	20°C	19.9 ± 0.54		69	
sod-5 [3]	25°C	12.5 ± 0.48	-22	89	<0.001
sod-5 [4]	25°C	12.7 ± 0.21		75	

sod-5 [5]	25°C	12.9 ± 0.31	-24	59	<0.0001
sod-5 [7]	20°C	19.3 ± 0.66		43	
sod-1 sod-5 [4]	25°C	11.9 ± 0.18	-6	72	<0.05
sod-1 sod-5 [5]	25°C	11.9 ± 0.18	-16	57	<0.001
sod-2; sod-3 [5]	25°C	16.8 ± 0.46		60	
sod-2; sod-3 [6]	25°C	17.4 ± 0.47		58	
sod-1 sod-5; sod-4 [5]	25°C	14.5 ± 0.40	-15	60	<0.001
sod-1 sod-5; sod-4 [6]	25°C	13.6 ± 0.33	-19	58	<0.0001

[a] Days ± SEM.
[b] Number of animals scored.
[c] Probability of being identical to wild-type control (log rank test).
[d] Data shown in Figure 3C.
[e] Data shown in Figure 2C.
[f] Data shown in Figure 3D.
[g] Data shown in Figure 2D.

Table S2

Effects of *sod* mutations on *daf-2(m577)* lifespan

Genotype [Trial number]	Temp.	Mean Lifespan[a]	% Change in lifespan	*n*[b]	*p*[c]
DATA IN FIGURES					
***daf-2* [2]**[d]	**20˚C**	**22.8 ± 0.77**		**24**	
***sod-1; daf-2* [2]**[d]	**20˚C**	**22.6 ± 0.31**		**54**	
***daf-2 sod-4* [2]**[d]	**20˚C**	**25.9 ± 0.95**	**+12**	**43**	**<0.01**
***daf-2* [3]**[e]	**25˚C**	**30.5 ± 0.45**		**58**	
***sod-2; daf-2* [3]**[e]	**25˚C**	**30.7 ± 0.50**		**60**	
***daf-2; sod-3* [3]**[e]	**25˚C**	**29.8 ± 0.48**		**60**	
ALL DATA					
daf-2 [1]	20˚C	24.0 ± 0.48		55	
daf-2 [2]	20˚C	22.8 ± 0.77		24	
daf-2 [3]	25˚C	30.5 ± 0.45		58	
daf-2 [4]	25˚C	30.6 ± 0.70		58	
daf-2 [5]	25˚C	34.3 ± 0.71		60	
daf-2 [6]	20˚C	25.7 ± 0.94		48	
sod-1; daf-2 [1]	20˚C	23.4 ± 0.64		48	
sod-1; daf-2 [2]	20˚C	22.6 ± 0.31		54	
sod-1; daf-2 [3]	25˚C	24.9 ± 0.51	-18	58	<0.0001
sod-1; daf-2 [4]	25˚C	27.6 ± 0.60	-10	58	0.0001
sod-2; daf-2 [3]	25˚C	30.7 ± 0.50		60	
sod-2; daf-2 [4]	25˚C	35.1 ± 0.55	+15	60	<0.0001
daf-2; sod-3 [1]	20˚C	23.4 ± 0.57		50	
daf-2; sod-3 [2]	20˚C	22.2 ± 0.60		34	
daf-2; sod-3 [3]	25˚C	29.8 ± 0.48		60	
daf-2; sod-3 [4]	25˚C	31.3 ± 0.62		59	
daf-2 sod-4 [1]	20˚C	26.8 ± 0.74	+12	53	<0.001
daf-2 sod-4 [2]	20˚C	25.9 ± 0.95	+12	43	<0.01
daf-2 sod-4 [3]	25˚C	32.5 ± 0.73	+7	63	<0.001
daf-2 sod-4 [4]	25˚C	34.3 ± 0.78	+12	60	<0.0001
sod-5; daf-2 [2]	20˚C	25.6 ± 1.03	+11	23	0.01
sod-5; daf-2 [4]	25˚C	31.9 ± 0.62		59	
sod-5; daf-2 [5]	25˚C	32.7 ± 0.82		55	
sod-5; daf-2 [6]	20˚C	21.2 ± 0.91	-18	46	0.003

[a] Days ± SEM.
[b] Number of animals scored.
[c] Probability of being identical to *daf-2(m577)* (log rank test).
[d] Data shown in Figure 3E.
[e] Data shown in Figure 2E.

Table S3

Effects of *sod-1* and catalase over-expression on lifespan (20˚C)

Genotype [Trial number]	Mean Lifespan[a]	% Change in lifespan	*n*[b]	*p*[c]
DATA IN FIGURES				
Wild type[d]	**18.6 ± 0.35**		**217**	
***wuls152 (sod-1)*[d]**	**22.6 ± 0.42**	**+21.5**	**337**	**<0.0001**
Wild type [15][e]	**19.0 ± 0.72**		**49**	
***wuls152 (sod-1)* [15][e]**	**25.3 ± 0.91**	**+24.9**	**45**	**<0.0001**
***wuls151 (ctl)* [15][e]**	**17.1 ± 0.70**	**-10**	**41**	**0.05**
***wuls151 (ctl) wuls152 (sod-1)* [15][e]**	**23.1 ± 0.88**	**+17.7, -8.7[f]**	**45**	**0.0002, 0.03[f]**
ALL DATA				
Wild type [2]	17.2 ± 0.79		24	
Wild type [3]	20.9 ± 0.85		25	
Wild type [5]	15.9 ± 0.64		25	
Wild type [6]	23.8 ± 1.61		14	
Wild type [7]	24.8 ± 0.77		21	
Wild type [8]	16.4 ± 1.13		11	
Wild type [9]	20.6 ± 1.33		12	
Wild type [10]	16.7 ± 1.65		11	
Wild type [11]	16.2 ± 1.76		11	
Wild type [12]	17.9 ± 0.93		20	
Wild type [13]	17.8 ± 1.26		15	
Wild type [14]	15.7 ± 0.64		28	
Wild type [15]	19.0 ± 0.72		49	
Wild type [16]	18.3 ± 0.80		24	
Wild type [17]	17.6 ± 0.70		22	
wuEx42 (rol-6) [1]	16.3 ± 0.77		25	
wuEx42 (rol-6) [4]	17.6 ± 0.64		74	
wuEx42 (rol-6) [15]	18.1 ± 0.90		48	
wuEx42 (rol-6) [16]	17.4 ± 0.53		43	
wuEx42 (rol-6) [17]	16.8 ± 0.98		18	
wuEx196 (rol-6) [16]	18.6 ± 0.48		51	
wuEx196 (rol-6) [17]	16.6 ± 0.45		44	
wuEx122 (sod-1) [16]	23.6 ± 0.96	+22	36	<0.0001
wuEx122 (sod-1) [17]	18.1 ± 0.67		44	
wuEx123 (sod-1) [16]	22.4 ± 0.73	+18	48	0.001
wuEx123 (sod-1) [17]	22.4 ± 0.88	+21	39	<0.0001
wuEx125 (sod-1) [6]	23.4 ± 1.7		27	
wuEx125 (sod-1) [8]	19.5 ± 1.16		17	
wuEx125 (sod-1) [11]	21.5 ± 1.07	+32.7	38	0.014
wuEx125 (sod-1) [16]	25.2 ± 1.34	+27	18	<0.0001
wuEx125 (sod-1) [17]	21.4 ± 0.78	+18	44	0.0007
wuIs152 (sod-1) [2]	24.3 ± 1.1	+41.3	24	<0.0001

wuIs152 (sod-1) [3]	24.5 ± 1.41	+17.2	29	0.018
wuIs152 (sod-1) [4]	24.5 ± 1.08	+39.2	22	<0.0001
wuIs152 (sod-1) [5]	27.2 ± 1.54	+71.1	23	<0.0001
wuIs152 (sod-1) [6]	23.7 ± 1.22		45	
wuIs152 (sod-1) [7]	27.4 ± 1.51	+10.5	44	0.0042
wuIs152 (sod-1) [8]	19.2 ± 1.56		9	
wuIs152 (sod-1) [9]	20.4 ± 1.49		19	
wuIs152 (sod-1) [10]	18.4 ± 1.19		21	
wuIs152 (sod-1) [11]	17.6 ± 0.79		22	
wuIs152 (sod-1) [12]	22.3 ± 1.22	+24.6	26	0.0043
wuIs152 (sod-1) [13]	18.3 ± 1.03		34	
wuIs152 (sod-1) [14]	19.1 ± 1.23	+21.7	19	0.0077
wuIs152 (sod-1) [15]	25.3 ± 0.91	+24.9	45	<0.0001
wuIs154 (sod-1) [1]	22.3 ± 1.22	+36.8	25	<0.0001
wuIs154 (sod-1) [3]	18.5 ± 0.94		25	
wuIs154 (sod-1) [4]	21.2 ± 0.79	+20.5	25	0.05
wuIs154 (sod-1) [5]	21.8 ± 1.09	+37.1	21	<0.0001
wuIs154 (sod-1) [6]	16.7 ± 1.19	-29.8	40	0.007
wuIs154 (sod-1) [7]	25 ± 1.73		25	
wuIs154 (sod-1) [8]	14.3 ± 0.92		18	
wuIs154 (sod-1) [9]	13.2 ± 0.88	-35.9	16	<0.0001
wuIs154 (sod-1) [10]	13.1 ± 0.68	-21.6	36	0.0179
wuIs154 (sod-1) [12]	19.5 ± 0.52		73	
wuIs154 (sod-1) [15]	21.2 ± 1.14	+10.4	50	0.014
wuIs151 (ctl) [2]	16.1 ± 0.76		22	
wuIs151 (ctl) [3]	16.5 ± 1.3	-21.1	15	0.0125
wuIs151 (ctl) [4]	18.6 ± 0.96		17	
wuIs151 (ctl) [5]	16.9 ± 0.66		22	
wuIs151 (ctl) [6]	10.4 ± 1.42	-56.3	35	<0.0001
wuIs151 (ctl) [7]	17 ± 1.03	-31.5	34	<0.0001
wuIs151 (ctl) [15]	17.1 ± 0.70	-10	41	0.05
wuIs151 (ctl) wuIs152 (sod-1) [7]	21 ± 2.21	-23.4[f]	22	0.01[f]
wuIs151 (ctl) wuIs152 (sod-1) [9]	20 ± 0.93		16	
wuIs151 (ctl) wuIs152 (sod-1) [10]	19.7 ± 0.69		50	
wuIs151 (ctl) wuIs152 (sod-1) [12]	18.6 ± 0.68	-16.6[f]	50	0.0034[f]
wuIs151 (ctl) wuIs152 (sod-1) [15]	23.1 ± 0.88	+17.7, -8.7[f]	45	0.0002, 0.03[f]

Lifespan was measured in the presence of FUdR, except for trials 2 and 3.
[a] Days ± SEM.
[b] Number of animals scored.
[c] Probability of being identical to wild-type or *rol-6* control (log rank test).
[d] Data shown in Figure 4F.
[e] Data shown in Figure 4G.
[f] *wuIs152 (sod-1) vs. wuIs151 (Ctl), wuIs152 (sod-1).*

Supplemental Experimental Procedures

Nematode strains

Mutant alleles and transgenic arrays used or generated in this study included LGI: *daf-16(mgDf50*), *sod-2(gk257)*; LGII: *sod-1(tm776)*, *sod-5(tm1146)*; LGIII: *daf-2(e1370)*, *daf-2(m577)*, *sod-4(gk101*); LGX: *sod-3(tm760)*. Unmapped integrated arrays: *wuIs54* [*sod-1::gfp*], *wuIs56* [*sod-3::gfp*], *wuIs57* [*sod-5::gfp*], *wuIs72* [*sod-2::gfp*], *wuIs151* [*ctl-1 + ctl-2 + ctl-3*; *myo-2::gfp*], *wuIs152* [*sod-1*], *wuIs154* [*sod-1*]. Extrachromosomal arrays: *wuEx42* [*rol-6(su1006)*], *wuEx196* [*rol-6(su1006)*],*wuEx122* [*sod-1*], *wuEx123* [*sod-1*], *wuEx125* [*sod-1*]. All transgenic arrays contain the visible marker pRF4 *rol-6(su1006*) unless otherwise stated.

Oxidative stress resistance assays

Paraquat resistance assays: young adults were placed overnight on agar plates containing 40uM fluorodeoxyuridine (FUdR), and then put into microtiter wells with 100 ul of 40mM paraquat (Sigma 856177) in M9 buffer. Viability was assayed over a 20 hr period. Hyperoxia resistance assays: young adults were picked onto plates containing 40uM FUdR and placed under 60% O_2 (22˚C). Animals were briefly removed from the O_2 chamber to score viability every 2 to 3 days.

Lifespan measurements and statistics

Lifespan assays were performed as previously described (Gems et al. 1998), at either 20°C or 25°C (see Table S1-S3). Survivorship of populations was compared statistically using the log rank test, performed using JMP 7.0.1 (SAS, Cary NC, USA).

Construction of *C. elegans* transgenic lines

Reporter constructs for each of the five *sod* genes were generated by subcloning the respective *sod* gDNA PCR fragment into pPD95.77, resulting in fusion of GFP to the C terminus of the SOD protein (see Figure S1). An in-frame fusion and lack of mutations was verified by DNA sequencing of all plasmids. Primer sequences used for fusions:

sod-1

CCCAAGCTTGCCAGCTGAGCAAACAGGAG

GGGGTACCCCCTGGGGAGCAGCGAGAGCAATGACACC

sod-2

ACATGCATGCTGAATCCTACGGAAAGTGCC

GGGGTACCCCTTGCTGTGCCTTTGCAAAACG

sod-3

ACATGCATGCAGTTTTTCATTTTCGGTATCGAAAACC

GGGGTACCGGTTGTCGAGCATTGGCAAATCTCTCG

sod-4

ACATGCATGCGGAAAGGGTTTAAAACTACTCCTATGTTGCC

GGGGATCCGACGGTACCTGTCAAACAGATTATATG

sod-5

ACATGCATGCGGTTGAGTTTATTTGACTTTTGG

GGGGTACCCCTGCAGGAGCGGCAAGAGCAATGACTCC

For *sod-1* over-expression, a 4.2 kb *sod-1* gDNA PCR fragment was injected at 30 ng/ul. Primers were CCCAAGCTTGCCAGCTGAGCAAACAGGAG and GGCACAACATTTATGGCAGTTTGG. For catalase over-expression, an 11.2 kb PCR fragment containing all three catalase genes, *ctl-1, ctl-2* and *ctl-3* was injected at 20 ng/ul. Primers were GTCCAAATCGGAGGATCTCA and GATGACACTGGCTCCCTCAT. pRF4 *rol-6(su1006)* was used as a marker of transformation in all cases apart from the catalase over-expressing strain, where *myo-2::gfp* was used. All integrated lines were back-crossed at least five times to N2 before further study.

Survey of expression patterns in *sod::gfp* lines

One integrated *sod::gfp* transgenic line for each *sod* gene was characterized in detail at the L3 stage in a *daf-2(+)* background. The expression pattern was then confirmed in a second, independent line (in most cases also integrated). For strains with *sod::gfp* in *daf-2* or *daf-16; daf-2* mutant backgrounds, and for studies of expression in dauer larvae, a single line was studied. Identification of amphid neurons with GFP expression was assisted by staining with the fluorescent carbocyanine dye DiI.

Harvesting nematodes for biochemical assays

Synchronous cultures were initiated via alkaline hypochlorite lysis of gravid adults. Eggs were allowed to hatch overnight in S buffer at 17°C and resulting L1 larvae were grown on NGM plates seeded with K12 *E. coli*. At harvest, young adult worms were rinsed off the plates, washed with S buffer, and stored at -75°C until use. Dauer larvae were harvested as previously described (Houthoofd et al. 2002). For all assays, 3-4 replicate worm cultures were used.

SOD and catalase activity assays

SOD activity was measured using an assay involving the inhibition of superoxide-induced lucigenin chemiluminescence by SOD, as described previously (Lenaerts et al. 2002). Catalase activity was assayed at 25°C according to a standard method (Aebi 1984), adapted for use in microtiter plate format.

Isolation of protein extracts via homogenization and subcellular fractionation

Worm samples were homogenized in 2ml microcentrifuge tubes containing equal amounts of suspended worms, glass beads, and 50mM Na/K phosphate buffer, pH 7.8, using a Mini-Beadbeater (Biospec Products, Bartlesville, OK, USA) operated at 5,000 strokes/min for 1min. The resulting homogenate was diluted to 1% in Chaps, kept on ice for 15 min, then centrifuged at 14,000 rpm for 8 min at 4°C. This supernatant was saved and cleared by a second centrifugation step. Mitochondrial fractions were prepared by rupturing the nematodes with a polytron homogenizer (40s at 14,000 rpm) in MSM-buffer (220 mM mannitol, 10 mM sucrose, 5 mM MOPS, pH 7.4 with KOH) containing 0.2% BSA. These crude homogenates were centrifuged twice in MSM-buffer at 380 g (5 min) to remove debris and intact worms. The supernatant was then spun at 4,500 g (5 min) and the resulting mitochondrial pellet was washed twice in MSM-buffer without BSA (5 min, 4500 g). Debris pellets and supernatants were pooled and centrifuged for 30 min at 14,000 rpm, and the supernatant was retained as a cytosolic fraction.

Real-time RT-PCR

This was performed as previously described (Hoogewijs et al. 2008). RNA was extracted using the RNeasy Midi kit (Qiagen, Venlo, The Netherlands). All samples were treated

with DNase (Zymo Research, Orange, CA, USA). A NanoDrop ND 1000 spectrophotometer was used to analyze RNA concentration and purity. First strand cDNA was synthesized from 2 μg RNA using an oligo(dT) primer and Moloney murine leukemia virus reverse transcriptase (Fermentas, Vilnius, Lithuania) at 42°C for 1 hr. Quantitative RT-PCR was carried out using a Rotor-Gene 2000 centrifugal real-time cycler (Corbett Research, Mortlake, Australia) using the Platinum SYBR Green qPCR SuperMix-UDG (Invitrogen, Carlsbad, CA, USA) as previously described (Hoogewijs et al., 2008). A single melt peak for each reaction confirmed the identity of each PCR product. Each assay included a no-template control for every primer pair. Primer sequences available upon request.

The threshold cycle (Ct) values of the Rotor-Gene software (version 6.0) were determined for three replicate serial dilutions of defined amounts of linearized plasmid containing the cDNAs of *sod-1*, *sod-2*, *sod-3*, *sod-4* or *sod-5*. These Ct values were used to generate standard curves from which original *sod* mRNA copy numbers were derived for each worm sample. Relative *sod* mRNA levels were calculated as the percentage of the different *sod* mRNA copy numbers to the total copy numbers of all *sod* genes in a single sample (see Fig. S2). Differential *sod* gene expression of 3 replicate nematode samples was measured as described previously (Hoogewijs et al. 2008). The Ct values of each sample were exported to qBase Version 1.3.5 (Hellemans et al. 2007). All measurements were produced in duplicate, and for each primer set, reaction efficiency estimates were derived from standard curves that were generated using serial dilutions of a cDNA pool of all nematode samples. These were then used by qBase to transform the Ct values to relative quantities, which were normalized using the geometric mean of three reference genes identified by the geNorm 3.4 software (Vandesompele et al. 2002). To minimize inter-experimental variation, the normalized *sod* expression ratios were standardized by converting the expression levels into logarithmic values, divided by their standard deviation and multiplied by the mean standard deviation of the 3 replicate experiments. Subsequently, the mean standardized expression per nematode sample and its 95% confidence interval was calculated. Finally, all values were linearized again using a power function, and plotted in a graph. Differential gene expression was considered significant when the 95% confidence interval of the mean expression levels did not overlap.

In situ gel SOD activity assay

SOD activity was analyzed by non-denaturing gel electrophoresis and staining with nitro blue tetrazolium as previously described (Jensen and Culotta 2005).

Western blot analysis

Proteins from worm homogenates or subcellular fractions were separated on a 15% SDS-PAGE gel and transferred onto a nitrocellulose membrane by semi-dry blotting, according to standard procedures. Equality of protein load was determined using Memcode reversible protein dye (Pierce). The membrane was blocked with milk-PBST and incubated with primary antibodies. MnSOD (# S8060-10b, raised in rabbit against mouse MnSOD, 1/10000 dilution) and Cu/ZnSOD (# S8060-09b, raised in rabbit against human CuZn SOD, 1/5000 dilution) primary antibodies were from US Biologicals. Actin antibody was from Sigma (# A4700, produced in mouse; 1/1000 dilution). CytochromeC antibody was from Mitosciences (# MSA06; produced in mouse; 1/2000 dilution). Subsequent incubation with secondary HRP-conjugated antibody and Supersignal West Pico chemiluminescent substrate (Pierce) generated light that was recorded on chemiluminescence film. Secondary anti-rabbit (# A0545; produced in goat; 1/20000 dilution) or anti-mouse antibodies (#A0168; 1/4000 dilution) were from Sigma.

Measurements of reproduction and defecation

Reproductive schedule (distribution of progeny production over time) and overall fecundity was measured by placing groups of 3 worms on NGM plates, transferring them daily to fresh plates, and counting the resulting progeny. Defecation was measured by timing 2-3 defecation cycles of 14 different worms of each genotype.

Dauer formation assays

daf-2(m577) eggs were cultured at 23.5°C, and the proportion of dauer larvae scored 72 hours later.

Acknowledgements

This work was supported by grants from the Wellcome Trust (to D.G.), and Ghent University (GOA 12050101), the Fund for Scientific Research-Flanders (G.0025.06), the European Community (LSHM-CT-2004-512020) (to J.R.V.). P.B. acknowledges a grant from the Institute for the Promotion of Innovation by Science and Technology in Flanders (IWT). Some strains were obtained from the *Caenorhabditis* Genetics Center, which is supported by the National Institutes of Health National Center for Research Resources. We thank David Hoogewijs for assistance with mRNA level estimations, and Peter Piper, Jennifer Tullet and David Weinkove for useful discussion and comments on the manuscript.

References for Supplemental Experimental Procedures

Aebi, H. 1984. Catalase *in vitro*. *Methods Enzymol* **105**: 121-126.

Hellemans, J., Mortier, G., De Paepe, A., Speleman, F., and Vandesompele, J. 2007. qBase relative quantification framework and software for management and automated analysis of real-time quantitative PCR data. *Genome Biol* **8**: R19.

Hoogewijs, D., Houthoofd, K., Matthijssens, F., Vandesompele, J., and Vanfleteren, J.R. 2008. Selection and validation of a set of reliable reference genes for quantitative sod gene expression analysis in *C. elegans*. *BMC Mol Biol* **9**: 9.

Houthoofd, K., Braeckman, B., Lenaerts, I., Brys, K., De Vreese, A., Van Eygen, S., and Vanfleteren, J. 2002. Ageing is reversed, and metabolism is reset to young levels in recovering dauer larvae of *C. elegans*. *Exp Gerontol* **37**: 1015-1021.

Jensen, L.T. and Culotta, V.C. 2005. Activation of CuZn superoxide dismutases from *Caenorhabditis elegans* does not require the copper chaperone CCS. *J Biol Chem* **280**: 41373-41379.

Lenaerts, I., Braeckman, B., Matthijssens, F., and Vanfleteren, J. 2002. A high-throughput microtiter plate assay for superoxide dismutase based on lucigenin chemiluminescence. *Anal Biochem* **311**: 90-92.

Vandesompele, J., De Preter, K., Pattyn, F., Poppe, B., Van Roy, N., De Paepe, A., and Speleman, F. 2002. Accurate normalization of real-time quantitative RT-PCR data by geometric averaging of multiple internal control genes. *Genome Biol* **3**: RESEARCH0034.